The thermohaline driving mechanism of oceanic jet streams

by G. T. Csanady[1]

ABSTRACT

Worthington (1972a) advanced the hypothesis that winter cooling of the Gulf Stream south of New England is the cause of the Stream's winter intensification. That loss of buoyancy should result in increased velocity and transport in an oceanic jet stream seems at first paradoxical. However, if a pattern of thermohaline circulation should arise in the upper layers of the Stream, it could play a role similar to that of the Hadley circulation in the atmosphere, which drives the subtropical jet stream. This possibility is examined here with the aid of a two-layer model, with the light layer being only "nearly homogeneous."

Thermohaline circulation arises in the light layer because the heat loss per unit mass near the front is much greater than further away, partly because of greater surface heat transfer to the unmodified air mass, partly on account of lesser penetration of surface cooling above a shallow pycnocline. The circulation carries heat toward the front, as well as streamwise momentum. The long-term cumulative effect (over an entire winter) of the momentum transport is to create substantial convergence just south of the front, causing a deepening of the thermocline and leading to increased transport. Order of magnitude estimates suggest, however, that the thermohaline circulation in isolation is not strong enough to produce the observed effects. It appears that the strong anticyclonic curl of the wind stress-force over the light layer just south of the front is at least a contributory factor in Gulf Stream intensification.

1. Introduction

In a series of publications dealing with the circulation of the North Atlantic, Worthington (1959, 1972a,b, 1976, 1977) has challenged the widely accepted notion that the Gulf Stream system is entirely wind-driven. He was able to demonstrate from many observations that the Gulf Stream over its most intense portion south of New England generally intensifies in winter. The challenge to conventional wisdom comes in Worthington's postulate that strong surface cooling in winter is the *cause* of Gulf Stream intensification, i.e., that a thermal mechanism is partially responsible for driving the Gulf Stream. Worthington speaks of "anticyclogenesis" and of a "fresh charge of energy" that the Gulf Stream receives at the end of each (severe) winter. At first sight these ideas seem paradoxical because they suggest that buoyancy loss, a dissipative effect in the sense of reducing available potential

1. Woods Hole Oceanographic Institution, Woods Hole, Massachusetts, 02543, U.S.A.

energy, has the incidental effect of accelerating an oceanic jet stream, increasing its total transport and kinetic energy.

It was also shown by Worthington (1959, 1972b) that a pattern of circulation in the cross-stream plane is associated with winter cooling and the consequent formation of Eighteen Degree Water. This pattern is in some ways analogous to the atmospheric Hadley circulation which is known to maintain the subtropical jet stream (Palmén and Newton, 1969). The analogy is imperfect and not as helpful as it could be because the fundamental processes involved are not well understood. It suggests, however, the likelihood of coupling between horizontal advective transports of heat and streamwise momentum, both of which are carried northward by the Hadley circulation. Given differential surface cooling, in analogy with differential surface heating in the atmosphere, a similar process is conceivable in the layers of the Sargasso Sea above the main thermocline. Whether such a process could significantly influence Gulf Stream behavior, or whether its results would be at all similar to what is known to occur in the course of Gulf Stream winter intensification, cannot be decided, however, without further investigation.

A highly simplified version of this problem is investigated analytically below. The water mass of the Sargasso Sea participating in Eighteen Degree Water formation is modelled as a "nearly homogeneous" light layer of 400 m depth, overlying a stagnant, heavier water mass. The main density saltus between heavy and light fluid is taken to occur at an interface, as in other two-layer models. Small density variations, however, are also allowed in the light layer in order to represent the effect of surface cooling. The rate of cooling is taken to be high in a narrow band (20 km) just south of the Gulf Stream front, but to vary only slowly outside this band. The total extent of the cooling region is large both along-stream and across-stream, compared to Gulf Stream width.

The interface slopes upward toward the front, so that surface heat loss, already a maximum near the front, comes to be distributed over a shallow water column, and causes relatively rapid temperature drop in the first instance. Horizontal temperature and hence density gradients are thus established and give rise to thermohaline circulation in the cross-stream plane. Surface cooling also causes vigorous convection in the light layer and therefore leads to efficient vertical transfer of heat or momentum. Geostrophic equilibrium with the horizontal density gradient requires a vertical gradient of the streamwise velocity: the full development of this is prevented by the strong mixing so that the thermohaline circulation remains relatively strong.

The thermohaline circulation transports both heat and streamwise momentum into the near-frontal zone. The horizontal (advective) heat transport balances the excess heat loss in this zone and maintains the rate of temperature change at the value characteristic of the large outer cooling region. The coupled momentum trans-

port, however, is not counterbalanced and causes changes in interface shape, maximum velocity, and jet stream transport. The coupling between heat and momentum transports is an earth rotation effect, always present in similar semi-closed circulation cells as long as the eddy friction is viscositylike.

The effects of momentum advection on the near-frontal region can only be approximately assessed. This is done on the basis of the potential vorticity equation, formulated for the nearly homogeneous light layer, following individual fluid columns with their depth-averaged velocity. Such a formulation is the logical extension of the classical two-layer approach, in which vertical gradients of density or horizontal velocity are taken to vanish layer by layer, to the case when such gradients are present in the light layer. The advective momentum flux divergence in the near-frontal region is distributed in the simplest way consistent with external constraints. This results in an anticyclonic curl of the momentum flux force and a negative potential vorticity tendency. Although negligible in the short term, over a whole winter the cumulative change in potential vorticity is large enough to result in considerable deepening of the interface just south of the front, with effects similar to those observed to accompany the winter intensification of the Gulf Stream.

It all adds up to a pretty complicated story, difficult to present in a logical sequence. Before embarking on the model development, the phenomenon of Gulf Stream winter intensification is described in greater detail, together with Worthington's arguments relating to it. Then, the potential vorticity tendency equation is developed for a nearly homogeneous layer because this can be done with a minimum of restrictive assumptions. Then the heat balance of the light layer is considered and the principal forcing term of the problem, the nonuniform surface heat loss, discussed. The flow field is next resolved into a basic geostrophic flow and a perturbation field (the thermohaline circulation), equations are written down for the latter, and the physics of this circulation discussed in the context of the balance of *streamwise* vorticity. An approximate solution is found for the "outer" region, where cooling is more or less uniform, and the advective transports of heat and momentum into the frontal region calculated for given horizontal temperature gradient. The problem is closed by a quasi-steady state approximation in which the rate of cooling is supposed the same in the frontal region as outside, i.e., the temperature gradient constant (after a spinup period, not considered).

The calculations yield a relationship of the horizontal temperature gradient to the excess heat loss in the frontal region, supplied by horizontal advection. Also, a relationship is found between horizontal heat and momentum advection, perhaps the principal result of the theory (Eq. 62). The response of the frontal region to the momentum flux is exhibited by means of a simplified model, consisting of a near-frontal region of reduced (constant) potential vorticity, and an outer region where this quantity is unchanged.

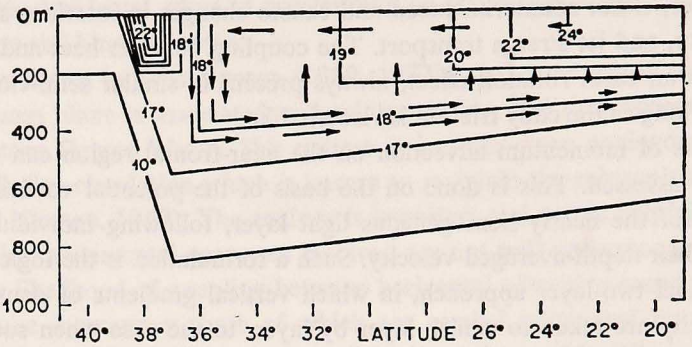

Figure 1. Meridional circulation in a transect of the Gulf Stream inferred from water mass formation. From Worthington (1972b).

2. Seasonal intensification of the Gulf Stream

The seasonal intensification of the Gulf Stream, documented by Worthington (1976) and attributed by him to surface cooling in winter (Worthington, 1959, 1972a,b; McCartney *et al.*, 1980) is associated with the following scenario. Cold air outbreaks from the North American continent bring about intense sea-to-air heat transfer over the Gulf Stream and just south of it. Consequent convective overturn of the upper few hundred meters of water in this region leads to the formation of a homogeneous water mass ("Eighteen Degree Water") which, over a stretch of the Gulf Stream some 2000 km long, escapes southward above the main thermocline. In replacement, warmer surface waters of the Sargasso Sea are drawn northward, resulting in a meridional circulation cell as illustrated schematically in Figure 1, from Worthington (1972b). At the northern (Gulf Stream) end of this cell the thermocline deepens in the course of the winter in such a way that the Gulf Stream transport relative to 2000 m increases by some 10 to 15 $\times$ 10^6 m^3 sec^{-1}.

The Gulf Stream "front" (intersection of free surface and interface) also shifts somewhat southward in the course of winter intensification. Figure 2, from Worthington (1976), is a schematic illustration of changes brought about by winter cooling in the position and shape of the interface. The type of observation on which this scheme is based is shown in Figure 3 here, after Worthington (1977), comparing temperatures in the Gulf Stream after a winter with many cold outbreaks with those after a mild winter. Disregarding a thin warm surface layer (presumably a consequence of surface layer advection) one finds loss of heat from the layers above 250 m. However, this is far more than compensated for by an increase of heat content at greater depth, associated with a depression of the main thermocline by some 200 m. Before a cold winter, 18° Water is not found deeper than 400 m south of the Gulf Stream, as it is not found below 400 m farther south, in the Sargasso Sea, at any time. Following a cold winter Eighteen Degree Water penetrates to 600 m depth south of the Gulf Stream, the isotherms sloping upward from here farther

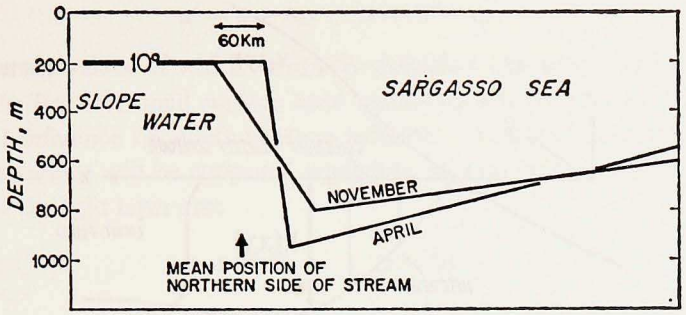

Figure 2. Schematic illustration of annual changes in Gulf Stream position and interface shape. From Worthington (1976).

southward, as shown in the schematic sketches of Figures 1 and 2. In other words, the meridional circulation induced by the cooling of the surface near the Gulf Stream delivers in the end more heat to the region near the front than necessary to make up for the deficit due to surface heat loss. Also, the cooling somehow has the incidental effect of accelerating a considerable water mass in a zonal (streamwise) eastward direction; a standard geostrophic calculation shows increased surface velocity and total transport to be associated with the deepened thermocline.

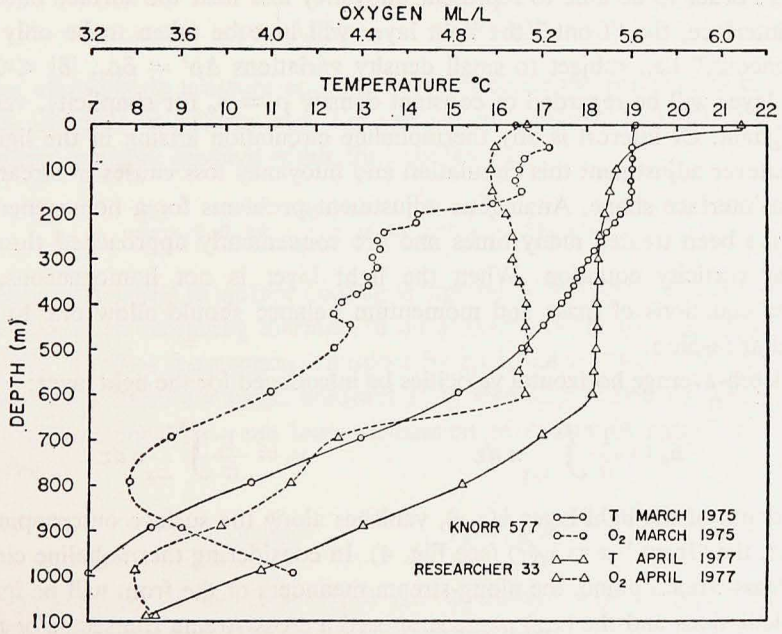

Figure 3. Temperature distribution (solid lines) just south of the Gulf Stream following a mild (○) and a severe (△) winter. From Worthington (1977).

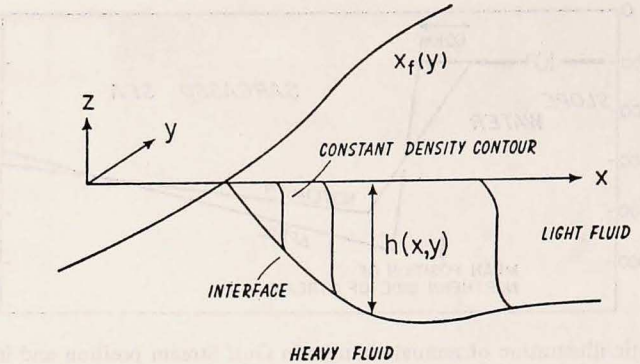

Figure 4. Coordinate system and "nearly homogeneous" light fluid layer, separated by an interface from heavy fluid. The interface $z = h(x,y)$ intersects the free surface, $z = 0$, along the "front", $x = x_f(y)$.

3. Motion of a "nearly homogeneous" light layer

An upper ocean jet stream and its associated front is often idealized by a two-layer model with all of the density change $\Delta\rho = \epsilon\rho_o$ supposed taking place across the interface, and the "light" and "heavy" layers homogeneous (e.g., Stommel, 1965). In order to be able to represent buoyancy loss near the surface outcropping of the interface, the "front," the light layer will here be taken to be only "nearly homogeneous," i.e., subject to small density variations $\Delta\rho' = \delta\rho_o$, $|\delta| << \epsilon$. The bottom layer will be regarded of constant density $\rho = \rho_o$ for simplicity, very deep, and stagnant. Of interest is any thermohaline circulation arising in the light layer, and whatever adjustment this circulation and buoyancy loss causes in stream velocity or in interface shape. Analogous adjustment problems for a homogeneous light layer have been treated many times and are conveniently approached through the potential vorticity equation. When the light layer is not homogeneous, *depth-averaged* equations of mass and momentum balance should allow one to proceed in a similar fashion.

Let depth-average horizontal velocities be introduced for the light layer:

$$u_a = \frac{1}{h}\int_{-h}^{o} u\,dz \qquad v_a = \frac{1}{h}\int_{-h}^{o} v\,dz\ . \tag{1}$$

The depth of the light layer $h(x,y)$, vanishes along the surface outcropping of the interface, the "front," $x = x_f(y)$ (see Fig. 4). In considering thermohaline circulation in the cross-stream plane, the along-stream meanders of the front will be ignored in later calculations and the (x,z) plane supposed a cross-stream transect. For the present, it is more illuminating to retain derivatives in the along-stream (y) direction.

Local velocity "anomalies" are now defined as

$$u' = u - u_a \qquad v' = v - v_a \tag{2}$$

the depth-average values of which vanish by definition. As already indicated by the upper limits in Eq. (1), small surface level variations will be ignored, because they have a trivial influence on depth-average velocities. Also, entrainment or detrainment at the interface will be supposed negligible, so that vertical velocities at these boundaries of the light layer are:

$$w = 0 \qquad (z = 0)$$

$$w = -\frac{\partial h}{\partial t} - u\frac{\partial h}{\partial x} - v\frac{\partial h}{\partial y} \qquad (z = -h)\ . \tag{3}$$

The density within the light layer will be written

$$\rho = \rho_o\,(1 - \epsilon + \delta) \tag{4}$$

with ϵ constant and δ variable, the latter reducing to zero far from the front:

$$\delta = 0 \qquad (x \to \infty)\ . \tag{5}$$

A positive value of δ corresponds to buoyancy loss near the front. The pressure field is supposed hydrostatic. In the stagnant bottom layer the pressure along the interface is therefore

$$p = \rho_o\, gh \qquad (z = -h) \tag{6}$$

having set atmospheric pressure equal to zero. Because the pressure is continuous across the interface, it follows from the hydrostatic equation and (4) and (6) that the horizontal pressure gradient within the light layer is:

$$\frac{\partial p}{\partial x} = \rho_o\,\epsilon g\frac{\partial h}{\partial x} - \rho_o\, g\frac{\partial}{\partial x}\int_{-h}^{z}\delta(z')dz'\ . \tag{7}$$

A light layer exposed to surface cooling is vigorously stirred by descending "thermals" analogous to ascending thermals in an atmospheric mixed layer (e.g., Deardorff, 1974). Vertical momentum transport by such convective turbulence will be represented by a relatively large, constant eddy viscosity, scaled by layer depth h and convection velocity w_*, see latter discussion of orders of magnitude. This is written here as:

$$\tau_x = \rho_o\, A\frac{\partial u}{\partial z} \qquad \tau_y = \rho_o\, A\frac{\partial v}{\partial z}\ . \tag{8}$$

Other components of the stress tensor are neglected.* The equations of motion and continuity for the light layer then take on the form:

* This refers to *eddy* momentum transfer. Horizontal momentum advection by the (weak) thermohaline circulation is considered in detail below.

$$\frac{\partial u}{\partial t} + u\frac{\partial u}{\partial x} + v\frac{\partial u}{\partial y} + w\frac{\partial u}{\partial z} = fv - \epsilon g\frac{\partial h}{\partial x} + g\frac{\partial}{\partial x}\int_{-h}^{z}\delta(z') + A\frac{\partial^2 u}{\partial z^2}$$

$$\frac{\partial v}{\partial t} + u\frac{\partial v}{\partial x} + v\frac{\partial v}{\partial y} + w\frac{\partial v}{\partial z} = -fu - \epsilon g\frac{\partial h}{\partial y} + g\frac{\partial}{\partial y}\int_{-h}^{z}\delta(z')dz' + A\frac{\partial^2 v}{\partial z^2} \tag{9}$$

$$\frac{\partial u}{\partial x} + \frac{\partial v}{\partial y} + \frac{\partial w}{\partial z} = 0 \ .$$

In performing depth-integration on these equations one must keep in mind that, for any function $\phi(x,z,\ldots..)$:

$$\int_{-h}^{o}\frac{\partial \phi}{\partial x}dz = \frac{\partial}{\partial x}\int_{-h}^{o}\phi\, dz - \frac{\partial h}{\partial x}\phi(x,-h,\ldots..) \ . \tag{10}$$

After some manipulations, depth integration results in:

$$\frac{du_a}{dt} = f v_a - \epsilon g\frac{\partial h}{\partial x} + \frac{1}{h}\frac{\partial P}{\partial x} + F_x + H_x$$

$$\frac{dv_a}{dt} = -f u_a - \epsilon g\frac{\partial h}{\partial y} + \frac{1}{h}\frac{\partial P}{\partial y} + F_y + H_y \tag{11}$$

$$\frac{dh}{dt} = -h\left(\frac{\partial u_a}{\partial x} + \frac{\partial v_a}{\partial y}\right)$$

where the depth integrated potential energy anomaly per unit mass is:

$$P = g\int_{-h}^{o}dz\int_{-h}^{z}\delta(z')dz' = -\int_{-h}^{o}z\delta(z)dz \tag{12}$$

and the total time derivative is defined following the depth-average motion:

$$\frac{d}{dt} \equiv \frac{\partial}{\partial t} + u_a\frac{\partial}{\partial x} + v_a\frac{\partial}{\partial y} \ . \tag{13}$$

The frictional and horizontal momentum flux forces in Eq. (11) are

$$F_x = \frac{1}{\rho_o}\frac{\tau_{wx} - \tau_{ix}}{h} \qquad F_y = \frac{1}{\rho_o}\frac{\tau_{wy} - \tau_{iy}}{h}$$

$$H_x = -\frac{1}{h}\frac{\partial}{\partial x}\int_{-h}^{o}u'^2\,dz - \frac{1}{h}\frac{\partial}{\partial y}\int_{-h}^{o}u'v'\,dz \tag{14}$$

$$H_y = -\frac{1}{h}\frac{\partial}{\partial x}\int_{-h}^{o}u'v'\,dz - \frac{1}{h}\frac{\partial}{\partial y}\int_{-h}^{o}v'^2\,dz$$

with τ_{wx}, τ_{wy} the components of the surface (wind) stress, τ_{ix}, τ_{iy} those of the interface stress. On taking curl on Eq. (11) one easily finds the form of the potential vorticity theorem applying to a nearly homogeneous layer:

$$\frac{d}{dt}\left(\frac{f+\frac{\partial v_a}{\partial x}-\frac{\partial u_a}{\partial y}}{h}\right)=-\frac{1}{h^3}\left[\frac{\partial h}{\partial x}\frac{\partial P}{\partial y}-\frac{\partial h}{\partial y}\frac{\partial P}{\partial x}\right]$$

$$+\frac{1}{h}\left[\frac{\partial F_y}{\partial x}-\frac{\partial F_x}{\partial y}+\frac{\partial H_y}{\partial x}-\frac{\partial H_x}{\partial y}\right]. \tag{15}$$

The total time derivative is again according to Eq. (13), i.e., following the depth-averaged flow.

The potential vorticity equation is of the same form as applies to a layer with vertically uniform density and horizontal velocity, except for two new source terms on the right: one, the Jacobian of the layer depth in $h(x,y)$ and the potential energy anomaly $P(x,y)$, and two, the curl of the horizontal momentum flux force, $\mathbf{H}(H_x,H_y)$. With buoyancy loss due to surface or interface heat flux the perturbation density field is principally depth-dependent, i.e., $P \cong P(h)$, so that the Jacobian should be small. This is not true if streamwise advection of density perturbations is significant, i.e., if surface heat loss is balanced partly by the divergence of the streamwise advective heat flux. In the present paper it is attempted to account for the observed facts on the basis of the hypothesis that it is principally the cross-stream advection that balances any excess heat loss, and the influence of the first term on the right of (15) is not further discussed. On the other hand, curl **H** arising as a result of thermohaline circulation is discussed and shown below to be an important influence on the distribution of potential vorticity.

The curl of the net stress force acting on the light layer, $\mathbf{F}(F_x,F_y)$ is also potentially important. Simple models of its effects on a homogeneous light layer have been discussed elsewhere (Csanady, 1977, 1980), and these serve as a first order guide to what one might expect from curl **H**. The curl of viscositylike interface stress is generally positive, tending to destroy anticyclonic vorticity of the jet stream. Its effect on the light layer is then to "flatten" the interface, i.e., to cause it to relax toward its ultimate horizonal equilibrium position. The curl of the wind stress (divided by layer depth h) may, on the other hand, well be negative or anticyclonic, and large near the front where h varies relatively rapidly.

On account of the stability dependence of the air-sea momentum transfer, wind stress in winter over the Gulf Stream is strongly anticyclonic and is conceivably an important factor in bringing about the changes accompanying winter intensification. Behringer *et al.* (1979) have discussed this effect and some of its consequences for the North Atlantic circulation. Here attention will be focussed on the alternative possibility that similar results are produced by a negative curl of the momentum flux force, **H**. If buoyancy loss, and the consequent cross-stream thermohaline circulation were to generate a sufficiently large negative curl **H**, the resulting thermocline deepening and jet intensification would indeed be thermally driven, more or

less as postulated by Worthington. The calculations that follow attempt to determine whether this is likely to be the case or not.

4. Distribution of heat loss

The temperature perturbation in the light layer resulting from surface heat loss will be denoted $\theta(x,y,z,t)$, with $\theta \to 0$ as $x \to \infty$, far from the front and the cooling region. The temperature field will be taken to be subject to the equation:

$$\frac{\partial \theta}{\partial t} + u\frac{\partial \theta}{\partial x} + v\frac{\partial \theta}{\partial y} + w\frac{\partial \theta}{\partial z} = K\frac{\partial^2 \theta}{\partial z^2} \tag{16}$$

with K an eddy conductivity. Horizontal eddy transfer of heat has been neglected, see later remarks. For the purposes of the present calculations the surface heat flux $q_o\,(x,y)$ will be supposed given:*

$$K\frac{\partial \theta}{\partial z} = -\frac{q_o}{\rho_o c_p} \qquad (z=0) \tag{17}$$

where c_p is specific heat of sea water. The interface is supposed insulating:

$$\nabla h \cdot \nabla \theta = 0\ . \tag{18}$$

Given the usual small interface shapes this is to a high degree of approximation:

$$\frac{\partial \theta}{\partial z} \cong 0 \qquad (z=-h)\ . \tag{18a}$$

The layer average temperature is

$$\theta_a = \frac{1}{h}\int_{-h}^{o} \theta(z)\,dz \tag{19}$$

which differs from the local temperature by the anomaly:

$$\theta' = \theta - \theta_a\ . \tag{20}$$

Depth integration of Eq. (16) now yields:

$$\frac{d\theta_a}{dt} = -\frac{q_o}{\rho_o c_p h} - \frac{1}{h}\frac{\partial}{\partial x}\int_{-h}^{o} u'\theta'\,dz - \frac{1}{h}\frac{\partial}{\partial y}\int_{-h}^{o} v'\theta'\,dz \tag{21}$$

where the total time derivative is as defined in Eq. (13), i.e., following the depth-averaged motion. Moving with the depth-average, or "fluid column" velocity (u_a,v_a), the layer average temperature θ_a drops owing to surface heat loss, except insofar as the divergence of horizontal heat transport compensates. The advective contribu-

* In order to avoid the complexities involved in a more accurate formulation. The sea-air temperature difference is large in cold outbreaks over the Gulf Stream and is relatively little influenced by the small sea surface temperature variations south of the Stream.

tion to the heat transport is determined by the velocity and temperature anomalies (u',v') and θ', i.e., it constitutes heat transport across vertical surfaces moving with the column velocity (u_a,v_a).

The forcing term in Eq. (21) is the kinematic surface heat flux $q_o/\rho_o c_p$, divided by layer depth h. This varies mainly in the cross-stream direction for two reasons: one, heat transfer from warm water to cold, dry air is largest where the unmodified air first encounters the stream, two, layer depth increases with distance from the front.* Most of the surface heat flux is readily shown to be latent heat of evaporation (Bunker and Worthington, 1976). The variation of evaporation rate with fetch in this situation is discussed in standard texts dealing with micrometeorology (Sutton, 1953; Brutsaert, 1982). Owing to the buildup of a moist inner boundary layer the evaporation rate decreases, although only slowly, about as $x^{-0.11}$, with x being the fetch. The charts of Bunker and Worthington (1976) vividly illustrate the cross-stream heat flux variation inferred from ship reports of sea-air temperature difference and wind speed.

Close to the front light layer depth varies linearly with cross-stream distance, and is thus the more important source of variability in q_o/h. This, however, is confined to a relatively short distance from the front, of the order of the internal radius of deformation, which in all such front-jet problems scales the variation of layer depth with distance from the front. The along-stream scale of surface heat loss (q_o) variations is determined mainly by the size of weather systems, and is large compared to the internal radius of deformation.

A (nearly) uniform value of q_o/h thus prevails over most of the formation area of Eighteen Degree Water, excepting only a narrow band south of the Gulf Stream front. The corresponding simple solution of Eq. (21) is a uniform rate of temperature drop, $d\theta_a/dt$, almost everywhere, with negligible divergence of total horizontal heat transport, eddy plus advective. The larger value of heat loss per unit mass in a narrow boundary layer south of the front, however, generates cross-stream temperature contrasts in the first instance. These are readily shown to bring about thermohaline circulation and a significant advective heat transport toward the front. Given the narrowness of the excess heat loss region, a two-dimensional model neglecting along-stream variability should be a sufficiently accurate tool for calculating cross-stream circulation and heat or momentum transport. Correspondingly, as foreshadowed earlier, the density perturbations arising from surface heat flux will be supposed independent of the along-stream coordinate, $\delta = \delta(x,z)$.

5. The equations of thermohaline circulation

The flow field within the light layer will be regarded as a superposition of the

* The "warm core" of the Gulf Stream located just south of the front further enhances the cross-stream variation of sea-air heat transfer.

basic geostrophic flow along contours of constant layer depth h, and a weaker thermohaline circulation. The basic flow is taken to be:

$$v_o = \frac{\epsilon g}{f} \frac{\partial h}{\partial x} \ . \tag{22}$$

Although the potential vorticity of the layer evolves according to Eq. (15), it is supposed to remain of order f/h_o, which is the potential vorticity in the undisturbed layer far from the front. The along-stream basic velocity is then of order

$$v_o = 0(c) \tag{23}$$

with $c = (\epsilon g\, h_o)^{\frac{1}{2}}$, the "densimetric velocity." The cross-stream scale of variation is the radius of deformation,

$$R = \frac{c}{f} \ . \tag{24}$$

Let the order of the density perturbation be written:

$$\delta = 0(\lambda\epsilon) \qquad (\lambda << 1) \ . \tag{25}$$

The (perturbation) velocity of the thermohaline circulation will be designated (u_1,v_1). Eq. (25) implies that this is of order

$$(u_1,v_1) = 0(\lambda c) \tag{26}$$

if the horizontal scale of variation of δ is R, as follows from earlier remarks. The along-stream scale of variation of any parameter will be taken to be small of the second order:

$$\frac{\partial}{\partial y} = 0(\lambda^2 R^{-1}) \ . \tag{27}$$

The time scale of evolution of the intensified jet stream is reasonably supposed long compared to f^{-1}:

$$\frac{\partial}{\partial t} = 0(\lambda f) \ . \tag{28}$$

Because the vertical velocity w varies on the vertical scale of layer depth according to the boundary conditions (3), it is now readily shown from the continuity equation that:

$$w = 0\left(\frac{h_o}{R}\ \lambda c\right) \tag{29}$$

which is of order $\lambda^2 c$ or less. In view of vigorous convection, the Ekman number will be taken to be of order λ, or relatively large, see later discussion of typical magnitudes:

$$E \equiv \frac{A}{fh_o^2} = 0(\lambda) \ . \tag{30}$$

When these scale relationships are substituted into Eqs. (9), the balance of zeroth order terms in λ is as already written down in Eq. (22), while the first order terms yield:

$$\begin{aligned} 0 &= fv_1 + g\frac{\partial}{\partial x}\int_{-h}^{z} \delta(x,z')\,dz' + A\frac{\partial^2 u_1}{\partial z^2} \\ \frac{\partial v_o}{\partial t} &+ u_1\frac{\partial v_o}{\partial x} = -fu_1 + A\frac{\partial^2 v_1}{\partial z^2} \ . \end{aligned} \tag{31}$$

Note here that the depth-average velocity (u_a,v_a) is the sum of $(0,v_o)$ and the depth-average of (u_1,v_1). To zeroth order in λ the potential vorticity equation (15) only contains $\partial v_o/\partial x$ on the left, and its right-hand side vanishes.

Equations (31) describe thermohaline circulation generated by the density perturbations $\delta(x,z)$. To focus on such circulation in isolation, wind and interface stresses will be supposed absent. The surface and interface boundary conditions are then

$$A\frac{\partial u_1}{\partial z} = A\frac{\partial v_1}{\partial z} = 0 \qquad (z = 0, -h) \ . \tag{32}$$

The eddy conductivity will be supposed to be of the same relatively high order as the eddy viscosity:

$$\frac{K}{fh_o^2} = 0(\lambda) \ . \tag{33}$$

It is now readily seen that the leading terms of the heat conduction equation (16) are of order $\lambda f\theta$, and consist of only

$$\frac{\partial \theta}{\partial t} + u_1\frac{\partial \theta}{\partial x} = K\frac{\partial^2 \theta}{\partial z^2} \ . \tag{34}$$

Horizontal eddy diffusion and vertical advection are both of a smaller order. To connect the heat conduction equation and the equations of motion (31) the density perturbation δ is supposed to depend linearly on the excess temperature θ:

$$\delta = -\alpha\theta \qquad (\alpha = \text{constant}) \ . \tag{35}$$

The thermal expansion coefficient will be understood to contain an allowance for salt residue left upon evaporation, see later remarks.

Differentiating the first of Eqs. (31) with respect to z one finds

$$0 = f\frac{\partial v_1}{\partial z} + g\frac{\partial \delta}{\partial x} + A\frac{\partial^3 u_1}{\partial z^3} \ . \tag{36}$$

A more general form of this equation serves as a useful guide to intuition. When

vertical velocities are of the same order as u_1, and when the time-scale of variation is not necessarily long, the linearized tendency equation for the streamwise (y) component of the vorticity, η, is (e.g., Chandrasekhar, 1961):

$$\frac{\partial \eta}{\partial t} = f \frac{\partial v_1}{\partial z} + g \frac{\partial \delta}{\partial x} + A \nabla^2 \eta \tag{37}$$

where

$$\eta = \frac{\partial u}{\partial z} - \frac{\partial w}{\partial x} .$$

This reduces to Eq. (36) under the approximations made above. The term containing the horizontal density gradient may be thought of as a source-term for the vorticity component η. When the scales of motion are such that the Coriolis force term is unimportant, (e.g., in a line thermal) the source term can only be balanced if either η is increasing, or if there is already distributed y-component vorticity present. In other words, a circulation in the (xz) plane must arise. Physically, the effect is simply due to the tendency of light fluid to overflow heavy fluid, or vice versa, heavy fluid to underflow light. In the system illustrated in Figure 4, buoyancy loss causes δ to increase toward the front, implying a tendency for counterclockwise circulation in the light layer (negative streamwise vorticity).

Earth rotation allows the vorticity tendency due to horizontal density variation to be balanced by the planetary vortex "tilting" term, $f\partial v_1/\partial z$. In meteorology, such a balance, between the first two terms in Eq. (36), is known as the thermal wind equation. However, with eddy friction significant, a three-way balance develops between the terms in Eq. (36), meaning that some circulation is present in the xz plane in steady state. The relative importance of the eddy friction term is measured by the Ekman number A/fh_o^2. According to Eq. (30), this is of order λ, so that the eddy friction term is of the same order as the other two. There is therefore every reason to expect thermohaline circulation to arise in the light layer.

The above vorticity tendency balance and its role in maintaining cross-stream circulation near a front has been further discussed in the illuminating series of recent numerical studies by Kao and his collaborators (Kao *et al.*, 1978; Kao, 1980, 1981).

6. Temperature distribution in the outlying region

The horizontal advection term in Eq. (34) couples the temperature and flow fields. It is not apparent how an analytical solution for the coupled set of equations could be obtained in the general case. However, an approximate solution may be found describing the circulation outside the narrow region of excess cooling near the front. From such a solution the horizontal transport of heat and momentum into the frontal zone may be calculated. This should allow one to assess the response of a jet stream to buoyancy loss in an approximate, yet quantitative, manner.

Following earlier discussion, the "outlying region" will be taken to be most of the Eighteen Degree Water formation area, outside the narrow "frontal zone" where excess cooling takes place. In the outlying region the variation of horizontal heat transport is on a scale much larger than R, and Eq. (21) becomes to the lowest order

$$\frac{d\theta_a}{dt} = \frac{\partial\theta_a}{\partial t} + u_a\frac{\partial\theta_a}{\partial x} = -\frac{q_o}{\rho_o c_p h} \ . \tag{38}$$

As in similar diffusion problems (e.g., Taylor, 1954), the temperature distribution in this region is plausibly expected to be a superposition of the column temperature $\theta_a(x,t)$ and a perturbation which is only a function of z:

$$\theta = \theta_a(x,t) + \theta'(z) \ . \tag{39}$$

The earlier definition of θ_a implies that

$$\int_{-h}^{o} \theta'(z)dz = 0 \ . \tag{40}$$

Noting that also $u_1 = u_a + u'$, substituting into Eq. (34) and using Eq. (38) one finds

$$-\frac{q_o}{\rho_o c_p h} + u'\frac{\partial\theta_a}{\partial z} = K\frac{\partial^2\theta'}{\partial z^2} \ . \tag{41}$$

By integration with respect to depth one readily verifies that the Ansatz of Eq. (39) is consistent with the boundary conditions (17) and (18). Integrating Eq. (41) twice with respect to z one finds the distribution $\theta'(z)$:

$$\theta'(z) = \frac{\partial\theta_a}{\partial x}\int_{-h}^{z} dz' \int_{-h}^{z'} \frac{u'(z'')}{K}\,dz'' - \frac{q_o}{\rho_o c_p K h}\left(\frac{z^2}{2} + hz\right) + \theta_r \tag{42}$$

where θ_r is a reference temperature, which must be chosen so as to satisfy Eq. (40). In calculating the horizontal heat transport, the integral in the second term of Eq. (21), θ_r drops out because the depth integral of u' vanishes by definition:

$$\frac{q_H h}{\rho_o c_p} \equiv \int_{-h}^{o} u'\theta'\,dz = \frac{\partial\theta_a}{\partial x}\int_{-h}^{o} u'(z)\,dz \int_{-h}^{z} dz' \int_{-h}^{z'} \frac{u'(z'')}{K}\,dz''$$

$$-\frac{q_o}{\rho_o c_p K h}\int_{-h}^{o} u'(z)\left(\frac{z^2}{2} + hz\right)dz \ . \tag{43}$$

The last result may be conveniently written in terms of the partial layer transport:

$$U(z) = \int_{-h}^{z} u'(z)\,dz \ . \tag{44}$$

It should be noted that $U(0) = 0$. Eq. (43) is now:

$$\frac{q_H h}{\rho_o c_p} = -\frac{1}{K}\frac{\partial \theta_a}{\partial x}\int_{-h}^{o} U^2(z)\,dz + \frac{q_o}{\rho_o c_p K h}\int_{-h}^{o}(h+z)U(z)\,dz\ . \qquad (45)$$

The second term on the right will be shown to be small compared to the first. The main contribution to the temperature anomaly $\theta'(z)$, neglecting θ_r and the term proportional to q_o in Eq. (42), may then be thought to arise as a balance between the tendency of nonuniform horizontal advection to distort the temperature profile by bringing in warm fluid at the top, cold fluid at the bottom, and vertical mixing, which tends to even out temperature differences. Problems involving such a balance between advection and diffusion have been discussed many times in the literature, following pioneering work by Taylor (1954). As Taylor has shown, and as is clear here from Eq. (42), the net result in a vertically confined fluid is quasi-diffusive transport down the gradient of the transported quantity, temperature in the present instance.

A comparison of the result, Eq. (42), with the Ansatz, Eq. (39), shows that the two are consistent provided that $u'(z)$, h, K and q_o are all independent of x. In the outlying region of the system considered here this should be true to zeroth order in the ratio of scales R/L, where L is the cross-stream dimension of the Eighteen Degree Water formation area.

To render Eq. (45) useful, it is necessary to express $u'(z)$ in terms of the parameters characterizing the temperature field.

7. Velocities and momentum transport

In the outlying region the layer depth is more or less constant by hypothesis, nearly equal to the equilibrium depth h_o, so that the terms containing derivatives of the basic flow velocity v_o vanish in Eqs. (31). Given a temperature distribution of the form of Eq. (39) these equations then reduce to:

$$0 = fv_1 - \alpha g(z+h)\frac{\partial \theta_a}{\partial x} + A\frac{\partial^2 u_1}{\partial z^2}$$

$$0 = -fu_1 + A\frac{\partial^2 v_1}{\partial z^2}\ . \qquad (46)$$

Boundary conditions at surface and interface have already been stated in Eqs. (32). The solutions of Eqs. (46), subject to boundary conditions (32) are standard: in a deep layer they consist of Ekman spirals at top and bottom, and geostrophic flow with a constant velocity gradient $\partial v_1/\partial z$ in the interior. In the present case the Ekman number is not small enough to suppose such a resolution automatically. The velocity distribution may be written as:

$$\frac{u_1}{v_{go}} = C_1 e^{z/D}\cos z/D + C_2 e^{z/D}\sin z/D + C_3 e^{-z/D}\cos z/D$$

$$+ C_4\, e^{-z/D} \sin z/D$$

$$\frac{v_1}{v_{go}} = \frac{(z+h)}{h} - C_2\, e^{z/D} \cos z/D + C_1\, e^{z/D} \sin a/D + C_4\, e^{-z/D} \cos z/D \tag{47}$$

$$- C_3\, e^{-z/D} \sin z/D$$

where C_j, $j = 1,2,3,4$ are integrations constants to be determined from the boundary conditions, v_{go} is surface geostrophic velocity perturbation:

$$v_{go} = \frac{\alpha g h}{f} \frac{\partial \theta_a}{\partial x} \tag{48}$$

and D is Ekman depth

$$D = (2Af^{-1})^{\frac{1}{2}} = (2E)^{\frac{1}{2}} h \ . \tag{49}$$

The constants C_j are functions of the depth to Ekman depth ratio:

$$C_j = \text{func}(h/D) \ . \tag{50}$$

These constants are in principle, readily calculated, although in practice the calculation involves a tedious amount of algebra.

For the purposes of order of magnitude estimates satisfactory approximations to the integrals in Eq. (45) may be obtained as follows. From the second of Eqs. (46) and the boundary conditions one finds

$$\int_{-h}^{o} u_1\, dz = 0 \tag{51}$$

so that $u_1 = u'$, there being no contribution from u_1 to u_a. From the same equation it also follows that

$$U(z) = \int_{-h}^{z} u_1\, dz = \frac{A}{f} \frac{\partial v_1}{\partial z} \ . \tag{52}$$

Even in a layer only moderately deep (h/D about 3, say) the value of $\partial v_1/\partial z$ at mid-depth is nearly equal to the thermal wind, so that in order of magnitude

$$U(z) \sim \frac{A\alpha g}{f^2} \frac{\partial \theta_a}{\partial x} \ . \tag{53}$$

Consequently, the integrals in Eq. (45) may be estimated to be

$$\int_{-h}^{o} U^2\, dz = \gamma_1 \frac{A^2\alpha^2 g^2}{f^4} \left(\frac{\partial \theta_a}{\partial x}\right)^2 h$$

$$\int_{-h}^{o} (h+z) U(z) dz = \gamma_2 \frac{A\alpha g}{f^2} \frac{\partial \theta_a}{\partial x} h^2 \tag{54}$$

where γ_1 and γ_2 are less than 1, perhaps typically ½ and ¼ for h/D around 3, and

become smaller with reducing h/D.

Another integration of Eq. (52) yields

$$v_1 = \frac{f}{A}\int_{-h}^{z} U(z')dz' + v_i \tag{55}$$

where v_i is the streamwise velocity perturbation at the interface, $z = -h$. In view of Eq. (51), the horizontal momentum transport may now be written as:

$$m \equiv \int_{-h}^{0} u'v'\,dz = \frac{f}{A}\int_{-h}^{0} u_1\,dz \int_{-h}^{z} U(z')dz'$$

$$= -\frac{f}{A}\int_{-h}^{0} U^2(z)dz\ . \tag{56}$$

This contains the same integral as the horizontal heat transport, estimated in the first of Eqs. (54). However, while the sign of the heat transport varies with the temperature gradient $\partial\theta_a/\partial x$ (supposing the first term on the right of Eq. (45) to dominate), the Coriolis parameter f is always positive in the northern hemisphere, resulting in a negative momentum transport, i.e., transport of streamwise momentum toward the front in the system considered here. The physical reason is that fluid moving toward the front in one leg of the ageostrophic cross-stream circulation is accelerated by the Coriolis force in the streamwise direction. In steady state, this acceleration is balanced by friction, but, given viscositylike eddy friction, that is only possible if fluid moving toward the front has a positive streamwise velocity perturbation. The converse applies to the return leg of the circulation, and the net result is transport of streamwise momentum into the stream, i.e., "up" the gradient of the basic geostrophic-flow velocity v_o. Similar effects have been discussed in greater detail elsewhere (Csanady, 1975).

8. Relationship of buoyancy and momentum transport

A closure of the problem is now possible on the following basis. Upon integration of Eq. (21) from the front over the entire region of excess cooling one finds, deleting y-derivatives:

$$\frac{q_H h}{\rho_o c_p} \equiv \int_{-h}^{0} u'\theta'\,dz = -\int_{x_f}^{x_o}\left(\frac{q_o}{\rho_o c_p} + h\,\frac{d\theta_a}{dt}\right)dx \tag{57}$$

where $x = x_o$ is the inner boundary of the outlying region. The integral on the right is the excess of the surface heat loss over the drop in heat storage within the frontal region. Prior to the establishment of a thermohaline circulation ($u' = 0$) this is zero, and temperature decreases more rapidly in the frontal than in the outlying region. As the temperature contrast increases, a thermohaline circulation develops and intensifies until a quasi-steady state is approached in which the horizontal tempera-

ture gradient no longer changes, i.e., $d\theta_a/dt$ is the same in the near-frontal and outlying regions. Writing for the area-average heat loss $q_o = \bar{q}_o$:

$$\frac{\bar{q}_o}{\rho_o c_p} = -h\,\frac{d\theta_a}{dt} \tag{57a}$$

one may also express (57) as:

$$q_H h = -\int_{x_f}^{x_o} (q_o - \bar{q}_o)\,dx\ . \tag{57b}$$

The horizontal heat transport may thus be estimated from the excess heat loss in the frontal region, and the width of that region. Quantitative estimates quoted below show that the excess $(q_o - \bar{q}_o)$ is of the same order as the average heat loss $\bar{q}_o$. The width of the frontal region, $x_o - x_f$, is, on the other hand, small compared to the cross-stream scale (L, say) of the Eighteen Degree Water formation area. Thus the horizontal heat transport $q_H h$ is only a small fraction of the total heat loss over the entire (frontal and outlying) region. In other words, most of the heat loss is reflected in the temperature drop.

With q_H determined, and the integrals estimated as per Eq. (54), Eq. (45) becomes a cubic equation for the temperature gradient:

$$\gamma_1\chi^3 - \gamma_2 B_z\chi = B_x \tag{58}$$

where nondimensional variables have been introduced as follows:

buoyancy gradient $$\chi = \frac{\alpha g}{f^2}\frac{\partial\theta_a}{\partial x}$$

buoyancy flux, horizontal $$B_x = \frac{\alpha g\, q_H}{\rho_o c_p f^2 K}$$

buoyancy flux, vertical $$B_z = \frac{\alpha g\, q_o}{\rho_o c_p f^2 K}\ .$$

In Eq. (58), the two eddy coefficients have been set equal, $K = A$. The factors γ_1 and γ_2 have been defined in Eq. (54); if $K \neq A$, $\gamma_1 \to \gamma_1 A^2/K^2$, $\gamma_2 \to \gamma_2 A/K$ in Eq. (58).

Given that the width of the excess cooling zone is of order R, and that the excess heat flux $(q_o - \bar{q}_o)$ in the frontal region is of the same order as the average heat flux $\bar{q}_o$, $B_z = 0(hB_x/R)$ and may be neglected in Eq. (58). Then:

$$\chi = (B_x\gamma_1^{-1})^{\frac{1}{3}}\ . \tag{59}$$

Writing for the nondimensional momentum flux:

$$M = \frac{m}{fhA} \tag{60}$$

one also has from Eq. (56)

$$M = -\gamma_1 \chi^2 \tag{61}$$

or, on substituting (59)

$$M = -\gamma_1^{\frac{1}{3}} B_x^{\frac{2}{3}} \ . \tag{62}$$

The dimensional relationship is also, directly from Eq. (45) with the second integral neglected (for the same reason that B_z was dropped above) and from Eq. (56):

$$\frac{q_H h}{\rho_o c_p m} = f^{-1} \frac{\partial \theta_a}{\partial x} \ . \tag{63}$$

The horizontal heat transport being supposed prescribed at the edge of the frontal region (to supply the excess heat loss within that region) the horizontal temperature gradient may be calculated from Eq. (59). Once this gradient is established in some spinup period, it induces vigorous enough cross-stream circulation to supply the heat needed in the frontal region to prevent more rapid than average rate of cooling. The result shows that the resemblance of Eq. (45) to a gradient heat transport law is illusory: the cross-stream heat flux is much more sensitive to the temperature gradient than a simple linear relationship implies. The physical reasons are that, (a) the velocity anomaly $u'(z)$ is proportional to the temperature gradient, (b) the temperature anomaly $\theta'(z)$ is generated by differential advection acting upon the cross-stream temperature gradient. Thus q_H comes to be proportional to $u' \cdot u' (\partial \theta_a / \partial x)$, which results in $q_H \sim (\partial \theta_a / \partial x)^3$.

Eqs. (59), (61), (62) and (63) parameterize horizontal transport of heat and momentum in terms of the horizontal temperature gradient, or eliminating that gradient, establish a relationship between transports of heat and momentum. The relationships also involve fluid properties, gravity, Coriolis parameter and the vertical eddy exchange coefficient. The last-named quantity is important: the estimates apply to a well-stirred light layer, the Ekman number being supposed relatively large. The most significant result is perhaps Eq. (62), supplying an explicit relationship between heat and momentum transport into the jet stream.

9. Frontal region response

It is now possible to analyze the response of the frontal region to the horizontal momentum transport. Figure 5 illustrates changes expected in the course of an entire winter. Suppose that a fluid column originally at $x = \xi_o$ constitutes the boundary between the frontal and the outlying regions. At a later time this column has moved to $x = x_o$, while the front has changed position from $x = 0$ to x_f. The stretching or squashing of the fluid columns between the front and the boundary column, and their cross-stream displacement, is subject to Eqs. (11), as well as to Eq. (15), derived from (11).

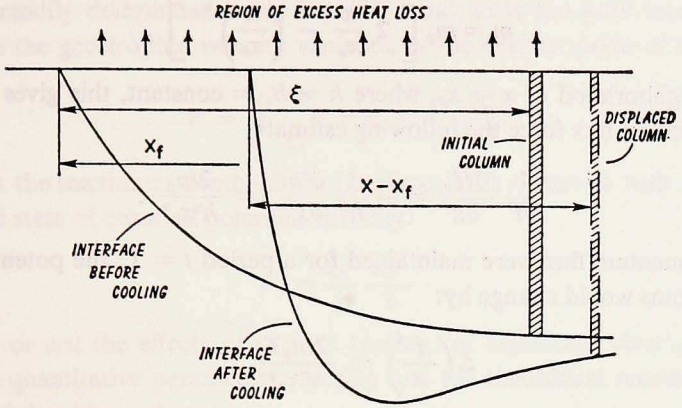

Figure 5. Schematic illustration of changes in frontal region brought about by excess heat loss: the front moves south of its initial position, the interface deepens. Individual fluid columns are displaced in a cross-stream direction, and are also stretched or squashed.

To the lowest order, Eqs. (11) reduce to the geostrophic balance of the basic flow, Eq. (22). Similarly, Eq. (15) shows that potential vorticity is conserved in a first approximation. However, the latter result applies to changes over short periods: the *cumulative* changes in potential vorticity, caused by the source terms on the right of Eq. (15) over a sufficiently long period may well come to be of the order of the initial potential vorticity. The question of interest here is whether the curl of the momentum flux force associated with the thermohaline circulation is large enough to bring this about.

The horizontal momentum flux force H_y is proportional to the cross-stream derivative of the momentum transport m. How this force is distributed within the frontal region cannot readily be determined. What the above calculations have shown is that at the outer edge of the frontal region the momentum transport has a certain negative value, estimated by Eq. (62). Furthermore, in this location horizontal heat transport and therefore also momentum transport have a broad maximum. At the front itself the momentum transport is zero, because it has to vanish with some power of fluid column depth. The momentum transport is therefore subject to the conditions:

$$\begin{aligned} m &= 0 && (x = 0) \\ m &= m_p \\ \frac{\partial m}{\partial x} &= 0 && (x = x_o) \end{aligned} \tag{64}$$

The simplest distribution $m(x)$ able to satisfy these conditions is the second degree polynomial:

$$m = m_p \left[2\frac{x}{x_o} - \left(\frac{x}{x_o}\right)^2 \right] . \tag{65}$$

In the neighborhood of $x = x_o$, where $h \cong h_o =$ constant, this gives for the curl of the momentum flux force the following estimate:

$$\frac{1}{h}\frac{\partial H_y}{\partial x} = -\frac{1}{h^2}\frac{\partial^2 m}{\partial x^2} = \frac{2m_p}{h^2 x_o^2} . \tag{66}$$

If the momentum flux were maintained for a period $t = T$, the potential vorticity of fluid columns would change by:

$$\Delta\left(\frac{f}{h}\right) = \frac{2m_p T}{h^2 x_o^2} . \tag{67}$$

A crude, but quantitatively realistic illustration of frontal region response to the horizontal momentum transport associated with thermohaline circulation should be obtained by supposing that all of the fluid columns between $x = x_f$ and x_o in Figure 5 have had their potential vorticity changed by the amount given by Eq. (67), while all other fluid columns have retained their initial potential vorticity, supposed constant at f/h_o. The zeroth order flow at the end of the cooling period T is then subject to

$$\begin{aligned} f + \frac{\partial v_o}{\partial x} &= f\frac{h}{h_1} && x_f \leqslant x \leqslant x_o \\ f + \frac{\partial v_o}{\partial x} &= f\frac{h}{h_o} && x_o \leqslant x \end{aligned} \tag{68}$$

$$\text{where} \quad \frac{f}{h_1} - \frac{f}{h_o} = \Delta\left(\frac{f}{h}\right) = \frac{2m_p T}{h_o^2 x_o^2} .$$

Substituting Eq. (22), a second order differential equation with constant coefficients is obtained for $h(x)$, to be solved subject to the boundary conditions:

$$\begin{aligned} &h,\ v_o && \text{continuous across } x = x_o \\ &h = 0 && (x = x_f) \\ &h = h_o && (x \to \infty) \\ &\int_o^{\xi_l} h(\xi)d\xi = \int_{x_f}^{x_l} h(x)dx && (x_l >> x_o) . \end{aligned} \tag{69}$$

The last condition expresses conservation of volume in the process of adjustment. The total of five conditions allow the determination of four constants arising in the solution of (68), two each for the two constant potential vorticity sections, and the frontal displacement x_f. From the resulting solution the geostrophic streamwise

velocity is readily determined using Eq. (22), and so is the total transport to the point where the geostrophic velocity vanishes, at the deepest point of the interface:

$$V = \int_{x_f}^{x_m} v_o\, h\, d_x = \frac{\epsilon g}{f}\,\frac{h_m^2}{2} \tag{70}$$

where h_m is the maximum depth of the interface. This contrasts with the transport in the initial state of constant potential vorticity:

$$V_o = \frac{\epsilon g}{f}\,\frac{h_o^2}{2}\ . \tag{71}$$

Whether or not the effects of surface cooling are significant clearly depends on the various quantitative parameters entering into the theoretical results, the estimation of which is addressed next.

10. Quantitative estimates

For the *annual* average surface heat flux over the formation region of the Eighteen Degree Water Worthington (1976) quotes a figure of 66 W m^{-2}. The peak *monthly* average winter heat flux over Marsden square 116 (off Chesapeake Bay) is given by Bunker and Worthington (1976) as about 500 W m^{-2}. Both these values are averages over areas of the order of 10^6 km^2. Over the central core of the Gulf Stream the average winter heat flux should be higher: using the $x^{-0.11}$ power law for evaporation rate, one estimates that over the first 1% of the evaporation area (order 10 km fetch in the Gulf Stream case) the heat flux is some 60% higher than the average, i.e., it is about 800 W m^{-2}. The annual and peak winter monthly rates are reconciled by noting that the period of intense cooling is about 1/8 year, or $0.4 \cdot 10^7$ s.

If one now supposes that the excess heat flux of 300 W m^{-2} applies to a 20 km wide strip, and that this is supplied by horizontal heat transport, the magnitude of the latter is estimated at

$$\frac{q_H h}{\rho_o c_p} = \int_{-h}^{0} u'\theta'\, dz = 1.5 \qquad ^\circ\text{C m}^2\,\text{s}^{-1}\ . \tag{72}$$

The typical temperature change may be calculated from the total heat loss in 1½ months, at the average rate of 500 W m^{-2}. Distributed over a 400 m deep layer this reduces the temperature by 1.2°C. Close to the front, where the depth is only half this great (say), and the surface heat loss 60% greater, the temperature drop would reach the average of 1.2°C within two weeks, in the absence of horizontal heat transport. Thus the quasi-steady state assumption made above should be realistic for the last 2/3 of the winter cooling period.

Much of the surface heat loss is due to evaporation, which leaves a residue of salt contributing to the negative buoyancy of the cooled skin at the water surface.

Without salinity changes the density change would be governed by the thermal expansion coefficient of water (Eq. 35). Given salt release attendent upon evaporation, the density change is somewhat greater. Around 20°C the value of α is about $2 \cdot 10^{-4}$ °C^{-1}: a value 25% higher will be used here to allow for salt residue formation.

Surface cooling evokes thermal convection, the intensity of which depends on vertical buoyancy flux and the depth of the mixed layer. Laboratory and atmospheric data show that the typical convection velocity is (Deardorff, 1974):

$$w_* = \left(\alpha g \frac{q_o}{\rho_o c_p} h_o \right)^{1/3} = 0.05 \text{ m s}^{-1} . \tag{73}$$

There is no fundamental difference between convection caused by heating from below or by cooling from above and the same formula may be used to estimate oceanic mixed layer convection. In the above estimate the average heat flux, $\bar{q}_o = 500$ W m^{-2} was used. Estimates of the vertical exchange coefficient in a convectively stirred layer may be taken from Deardorff and Willis (1975) and Willis and Deardorff (1978) and range from

$$\frac{K}{w_* h_o} = 0.08 \text{ to } 0.25 \tag{74}$$

or $K = 1.6$ to 5 m^2 s^{-1}. Thermohaline circulation contributes to stability by advecting warmer water at the top, colder at the bottom. Therefore a value for the exchange coefficient near the lower end of the above estimates will be adopted, $A = K = 2$ m^2 s^{-1}. Given $h_o = 400$ m, $f = 10^{-4}$ s^{-1} the Ekman number is then:

$$E \equiv \frac{A}{f h_o^2} = \frac{2}{16} = 0.125 . \tag{75}$$

All independent variables in the buoyancy transport versus temperature gradient relationship of Eq. (59) have now been estimated, the remaining fixed constants being $\rho_o = 1000$ kg m^{-3}, $c_p = 4188$ J kg^{-1} °C^{-1}, g $= 10$ m s^{-2}. The nondimensional horizontal buoyancy flux is, from these estimates:

$$B_x = 470 . \tag{76}$$

For the nondimensional temperature gradient Eq. (59) gives $\chi = 10$ or so, equivalent to the dimensional quantity:

$$\frac{\partial \theta_a}{\partial x} = 4 \cdot 10^{-5} \text{ °C m}^{-1} . \tag{77}$$

This is consistent with the earlier estimate of the typical temperature being 1.2°C, given a horizontal scale of 25 km. Given B_x, Eq. (62) supplies the estimate for the nondimensional momentum flux of about $M = -47$, and hence the dimensional momentum transport

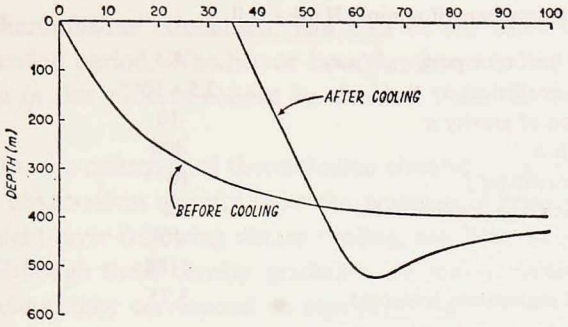

Figure 6. Results of model calculations on interface response to excess cooling. Two regions of different constant potential vorticity, and correspondingly of different curvature, are joined near inflection point at 75 km in "after cooling" shape.

$$m = -3.75 \text{ m}^3 \text{ s}^{-2} .$$

Distributed over depth, this is about $\overline{u'v'} \sim 0.01$ m^2 s^{-2}, suggesting that perturbation velocities are of order 0.1 m s^{-1}. The temperature gradient found above implies a thermal wind of 10^{-3} s^{-1}, i.e., an upper limit on the streamwise velocity variation over a column 400 m deep of about 0.4 m s^{-1}. These estimates justify the fundamental scaling assumptions contained in Eqs. (25) and (26).

Using now Eq. (67) with $T = 0.4 \cdot 10^7$ s, the potential vorticity drop is found to be nearly 50% of the original value f/h_o, resulting in a modified equilibrium depth $h_1 = 770$ m. Calculations according to Eqs. (68) and (69) also yield the southward movement of the front (35 km) and the detailed shape of the interface after the winter cooling period (Fig. 6). A maximum depth of about 520 m is reached some 30 km south of the displaced front, the interface sloping *upward* from there, in a southward direction. The geostrophic flow in this region is directed opposite to the stream, i.e., westward. The total eastward transport increases according to Eq. (70) by some 70%, the excess being returned in the westward flow region. The maximum jet velocity is only slightly higher (by 8%) than the value before cooling.

Given that only a 400 m deep layer participates in the cooling scenario by hypothesis, the calculated increase in transport is about $5 \cdot 10^6$ m^3 s^{-1}, comparable to the observed increase in the topmost layers alone. The southward movement of the front is also only about half of Worthington's estimate (see Fig. 2). Although the estimates made here are very crude, they suggest that thermohaline circulation makes an important contribution to Gulf Stream winter intensification, even if, standing alone, this mechanism may be insufficient to explain all of the observed facts. One point in favor of this explanation is that the thermohaline mechanism brings about anticyclogenesis on a horizontal scale of order R, i.e., a rather "tight" recirculation, which is observed and is otherwise difficult to explain.

Table 1. Parameters of oceanic Hadley cell.

kinematic heat transport, $q_H h/\rho_o c_p$	1.5	$°C\ m^2\ s^1$
expansion coefficient α	$2.5 \cdot 10^{-4}$	$°C^{-1}$
acceleration of gravity g	10	$m\ s^{-2}$
layer depth h	400	m
Coriolis parameter f	10^{-4}	s^{-1}
vertical exchange coefficient K_z	2	$m^2\ s^{-1}$
density ρ	10^3	$kg\ m^{-3}$
specific heat c_p	4188	$J\ °C^{-1}\ kg^{-1}$
calculated momentum transport	3.75	$m^3\ s^{-2}$

Nevertheless, it is relevant to note that wind stress is eastward and intense over the warm core of the Gulf Stream in winter, its curl high and anticyclonic (Behringer *et al.*, 1979). The force of this stress distributed over the light layer, $\tau_w/\rho h$, is large near the front for much the same reasons that make the excess heat loss large there: increased drag coefficient of cold air over warm water, and the more important effect, rapid variation of layer depth with cross-stream distance. A variation in eastward wind stress force, of 0.1 Pa divided by 400 m depth, over 20 km cross-front distance, gives the same rate of potential vorticity decrease as the horizontal momentum flux force estimated above. There are therefore strong reasons to suspect that the observed intensification is produced by a combination of cooling and sharp wind-stress force variation over the Stream. This would still be an air-sea interaction effect, legitimately described as "anticyclogenesis," as Worthington has postulated, but not solely a byproduct of thermohaline circulation and Eighteen Degree Water formation. By whatever mechanism the potential vorticity of the light layer is reduced, substantial deepening of the layer close to the front implies an upward-sloping interface further away, so that the increased transport is always returned in a narrow recirculation region, pretty much as envisaged by Worthington.

The principal parameters used in the calculation of light layer response to winter cooling are summarized in Table 1.

11. Discussion

The qualitative similarity of the "after cooling" interface shape in Figure 6 to Worthington's schematic illustration of observed winter response (Fig. 2 here) is clear, but it is important to note that this merely confirms the decrease in potential vorticity over a band of the light layer just south of the front.* Indeed, proceeding from the observational evidence, one can immediately conclude that such decrease takes place during a winter. Eq. (15), and other arguments made above, show that there are two likely causes for this, curl of the horizontal momentum flux force due

* Over and above the seasonal change of potential vorticity occurring over the Eighteen Degree Water formation area.

to a pattern of thermohaline circulation, and curl of the wind stress force, both acting for an extended period. Whether or how far thermohaline circulation plays an important role in this process cannot be decided from the empirical evidence alone.

The argument for the *existence* of thermohaline circulation is, on the other hand, fairly conclusive: observations directly show the presence of horizontal density contrasts within the light layer following winter cooling, see Worthington's illustrations quoted before. Although these density gradients are minor compared to those in the main thermocline, they correspond to significant vertical velocity gradients in geostrophic balance. However, in a mixed layer well stirred by convection, eddy friction is intense and disturbs geostrophic balance, so that a cross-stream thermohaline circulation should be present. The essence of this argument is that the Ekman number in a well-stirred layer is relatively large, and friction competes effectively with Coriolis force in balancing horizontal pressure gradients due to nonuniform density. Empirical evidence on the atmospheric boundary layer under convective conditions leaves little doubt that this is in fact the case also in an oceanic surface layer subject to intense cooling from above.

Given horizontal temperature differences and a pattern of thermohaline circulation, horizontal heat transport by this circulation is a plausible inference. Direct evidence for its existence is the observed near-uniformity of temperature change in the light layer, extending in particular to its shallow portion near the front, where surface heat loss is greatest. In the absence of horizontal heat transport, this region would cool substantially more, and temperature gradients would be greater than observed, unless, of course, along-stream advection of heat would compensate. This is an alternative possibility not examined here by hypothesis (Eq. 27).

The above calculations have shown that the across-stream circulation carries streamwise momentum toward the front, as it carries heat. One of the principal theoretical conclusions is Eq. (62), a simple power law formula connecting nondimensional momentum flux to buoyancy flux. A relationship between the two nondimensional fluxes should be expected from a simple dimensional argument. That the relationship should be a 2/3 power law follows from the third-power dependence of heat flux on temperature gradient, the physical causes of which were discussed earlier. Gulf Stream observations, however, do not provide direct evidence to support either the functional form of Eq. (62) nor verification that the constant in this equation is of order one.

It is therefore of some interest to examine the thermohaline circulation in the atmosphere at low latitudes, known as the Hadley circulation. This is in many respects analogous to the thermohaline circulation in a light layer discussed above in that it is driven by nonuniform heating from below, which also generates deep convection. The Hadley circulation transports heat and momentum northward, the momentum transport maintaining the subtropical jet stream, an atmospheric analog

Table 2. Parameters of atmospheric Hadley cell.

kinematic heat transport, $q_H h/\rho_o c_p$	$0.8 \cdot 10^5$	°C m² s⁻¹
expansion coefficient α	$3 \cdot 10^{-3}$	°C⁻¹
acceleration of gravity g	10	m s⁻²
layer depth h	10^4	m
Coriolis parameter f	$0.5 \cdot 10^{-4}$	s⁻¹
vertical exchange coefficient K_z	10^2	m² s⁻¹
density ρ	1.2	kg m⁻³
specific heat c_p	1050	J °C⁻¹ kg⁻¹
momentum transport	$4 \cdot 10^5$	m³ s⁻²

of the Gulf Stream. Palmén and Newton (1969) discuss Hadley circulation in considerable detail.

Heat and momentum transports by the Hadley circulation are known from observation and they may be compared with the predictions of Eq. (62). Palmén and Newton (1969) gives momentum flux in units of angular momentum transport, translatable into flux of eastward linear momentum on division by $2\pi\ a^2 \cos^2\phi$, where a is earth radius, ϕ latitude. In Table 2 here these transports are listed at 20° latitude, which presumably corresponds to the region of maximum heat and momentum flux for which Eq. (62) was derived. Other reasonably chosen atmosphere parameters are also listed in Table 2.

The nondimensional buoyancy flux in the atmospheric Hadley circulation is about $B_x = 10^6$ or three orders of magnitude greater than in the Gulf Stream model discussed above. Eq. (62) gives a corresponding nondimensional momentum flux, with $\gamma_1 = 0.5$, of $M = 0.8 \cdot 10^4$, which translates into a dimensional momentum transport of $0.4 \cdot 10^6$ m³ s^{-2}. This is about 50% higher than the observed value, or an estimate as close as one would expect to get using crude order of magnitude figures for atmospheric characteristics.

In this entire paper attention was focussed on horizontal heat transport, which actually plays a minor role in the redistribution of heat loss, most of the temperature change in the Eighteen Degree Water formation area being simply local response to cooling. The formation of this larger, slightly heavier water mass, and its adjustment to geostrophic equilibrium has not been touched upon. This aspect of the problem was recently studied by Stommel and Veronis (1980) who also examined the lower layer response to the formation of an intermediate-density water mass. Stommel and Veronis made their calculations on the basis of potential vorticity conservation, supposing an impulsive change of temperature over a considerable water mass. This is undoubtedly a good approximation in regard to the behavior of the larger cooled water mass. It leaves out of account, however, such effects of nonuniform cooling as were discussed above, especially the changes in potential vorticity south of the front.

It remains to comment on the likely role of hydrodynamic instability. Flow in geostrophic equilibrium with horizontal density gradients is well known to be unstable, and to evolve into intense jets, meanders and cutoff eddies. The degree of instability as expressed by the growth rate of the most unstable disturbance, however, depends on how strong a damping influence friction is. At a relatively high Ekman number the growth rate of disturbances becomes too slow for instability to manifest itself seriously. Antar and Fowlis (1981) have recently examined the stability of flow in a layer of fluid subject to a horizontal density gradient, under boundary conditions similar to those applied in the calculations above. On the basis of their results, at the high Ekman numbers characterizing a layer subject to vigorous convection one is justified in concluding that effects of instabilities are minor. This point of view is further supported by the observed fact that at low latitudes in the atmosphere heat and momentum transport is carried predominantly by the mean Hadley circulation, not by eddies (Palmén and Newton, 1969), so that there is precedent for the type of coupled heat and momentum transport by steady thermohaline circulation envisaged in calculations above.

Acknowledgments. The work described herein was supported at the Woods Hole Oceanographic Institution by the NASA Oceanic Processes Program, as part of a project entitled Warm Water Mass Formation. It was completed at the California Institute of Technology, with support from the Sherman Fairchild Scholarship Fund. I am grateful for the hospitality of Drs. N. H. Brooks and E. J. List at Caltech. Dr. M. S. McCartney, acting as a referee, kindly made useful suggestions. Contribution no. 5109 of the Woods Hole Oceanographic Institution.

REFERENCES

Antar, B. N. and W. W. Fowlis. 1981. Baroclinic instability of a rotating Hadley cell. J. Atm. Sci., *38,* 2130–2141.

Behringer, D., L. Regier and H. Stommel. 1979. Thermal feedback as a contributing cause of the Gulf Stream. J. Mar. Res., *37,* 699–709.

Brutsaert, W. H. 1982. Evaporation into the Atmosphere. D. Reidel Publishing Co., 299 pp.

Bunker, A. F. and L. V. Worthington. 1976. Energy exchange charts of the North Atlantic Ocean. Bull. Am. Meteor. Soc., *57,* 670–678.

Chandrasekhar, S. 1961. Hydrodynamic and Hydromagnetic Stability. Clarendon Press, Oxford, 652 pp.

Csanady, G. T. 1975. Lateral momentum flux in boundary currents. J. Phys. Oceanogr., *5,* 705–717.

—— 1977. Intermittent 'full' upwelling in Lake Ontario. J. Geophys. Res., *82,* 397–419.

—— 1980. Fronts near geostrophic equilibrium, *in* Proc. Second International Symposium on Stratified Flows, T. Carstens and T. McClimans, eds., Tapir Publishers, Trondheim, Norway, 40–71.

Deardorff, J. W. 1974. Three-dimensional numerical study of the height and mean structure of a heated planetary boundary layer. Boundary Layer Meteor., *7,* 81–106.

Deardorff, J. W. and G. E. Willis. 1975. A parameterization of diffusion into the mixed layer. J. Appl. Meteor., *14,* 1451–1458.

Kao, T. W. 1980. The dynamics of oceanic fronts, Pt. I: The Gulf Stream. J. Phys. Oceanogr., *10,* 483–492.

—— 1981. Addendum to the dynamics of oceanic fronts, Part I: The Gulf Stream. J. Phys. Oceanogr., *11*, 568–569.

Kao, T. W., H. P. Pao and C. Park. 1978. Surface intrusions, fronts and internal waves: a numerical study. J. Geophys. Res., *83*, 4641–4650.

McCartney, M. S., L. V. Worthington and M. E. Raymer. 1980. Anomalous water mass distributions at 55W in the North Atlantic in 1977. J. Mar. Res., *38*, 147–172.

Palmén, E. and C. W. Newton. 1969. Atmospheric Circulation Systems. Academic Press, New York, 603 pp.

Stommel, H. 1965. The Gulf Stream. University of California Press, Berkeley, 248 pp.

Stommel, H. and G. Veronis. 1980. Barotropic response to cooling. J. Geophys. Res., *85*, 6661–6666.

Sutton, O. G. 1953. Micrometeorology. McGraw Hill Publishing Co., 333 pp.

Taylor, G. I. 1954. The dispersion of matter in turbulent flow through a pipe. Proc. Roy. Soc., Ser. A., *223*, 446–467.

Willis, G. E. and J. W. Deardorff. 1978. A laboratory study of dispersion from an elevated source within a modeled convective planetary boundary layer. Atmos. Environment, *12*, 1305–1311.

Worthington, L. V. 1959. The 18° water in the Sargasso Sea. Deep-Sea Res., *5*, 297–305.

—— 1972a. Anticyclogenesis in the oceans as a result of outbreaks of continental polar air, *in* A tribute to Georg Wüst on his 80th birthday, A. L. Gordon, ed., Gordon and Breech, New York, 169–178.

—— 1972b. Negative oceanic heat flux as a cause of water mass formation. J. Phys. Oceanogr., *2*, 205–211.

—— 1976. On the North Atlantic Circulation. Johns Hopkins Press, Baltimore, Md., 110 pp.

—— 1977. Intensification of the Gulf Stream after the winter of 1976-77. Nature, *270*, 415–417.

Received: *5 August, 1981;* revised: *19 April, 1982.*